Structural Engineering and Mechanics, *Vol. 61, No. 6 (2017) 693-700*
DOI: https://doi.org/10.12989/sem.2017.61.6.693

Numerical modeling of concrete cover cracking due to steel reinforcing bars corrosion

Mohammad Javad Mirzaee[1a], Farshid Jandaghi Alaee[1b], Mohammad Hajsadeghi[2c] and Tadeh Zirakian[*3]

[1]*Department of Civil Engineering and Architecture, University of Shahrood, Shahrood, Iran*
[2]*School of Engineering Sciences, University of Liverpool, Liverpool L69 3BX, UK*
[3]*Department of Civil Engineering and Construction Management, California State University, Northridge, CA, USA*

(Received June 15, 2016, Revised October 22, 2016, Accepted November 6, 2016)

Abstract. Concrete cover cracking due to the corrosion of steel reinforcing bars is one of the main causes of deterioration in Reinforced Concrete (RC) structures. The oxidation level of the bars causes varying levels of expansion. The rebar expansions could lead to through-thickness cracking of the concrete cover, where depending on the cracking characteristics, the service life of the structures would be affected. In this paper, the effect of geometrical and material parameters, i.e., concrete cover thickness, reinforcing bar diameter, and concrete tensile strength, on the required pressure for concrete cover cracking due to corrosion has been investigated through detailed numerical simulations. ABAQUS finite element software is employed as a modeling platform where the concrete cracking is simulated by means of eXtended Finite Element Method (XFEM). The accuracy of the numerical simulations is verified by comparing the numerical results with experimental data obtained from the literature. Using a previously proposed empirical equation and the numerical model, the time from corrosion initiation to the cover cracking is predicted and then compared to the respective experimental data. Finally, a parametric study is undertaken to determine the optimum ratio of the rebar diameter to the reinforcing bars spacing in order to avoid concrete cover delamination.

Keywords: corrosion; concrete cover cracking; reinforced concrete structures; eXtended finite element method; service life

1. Introduction

The appearance of visible cracks is a trigger to execute an appropriate inspection, since most deterioration processes such as reinforcement corrosion for reinforced concrete are likely to result in concrete cover cracking. However, due to the high alkalinity of the concrete pores solution, a thin layer is formed surrounding steel reinforcing bars which protects them against corrosion (Broomfield 2007). In this case, the bars are called "Passive". This layer is unstable and disappears with decrease of pH. Carbonation of the concrete cover and the presence of sufficient chloride ions on the steel bars surfaces are the main causes for the protective layer disappearance and corrosion initiation (Zhao *et al.* 2011). The process of chloride ingress in saturated concrete has been investigated by previous researchers where a few models for chloride diffusion have been presented (Song *et al.* 2014, Tsao *et al.* 2015). The corrosion products diffuse into capillary voids in concrete. If the total amount of corrosion products is less than the porous zone volume, no additional stress is developed in concrete. This stage is known as free expansion. However, when the products volume exceeds that of the porous zone, expansive stress is developed in concrete surrounding the reinforcing bars; the more corrosion products, the higher stress. Finally, once the stress exceeds tensile strength of concrete, cracking initiates (Liu 1996). Therefore, RC structures which are exposed to aggressive environments are prone to fail before reaching the end of their service lives (Zhao *et al.* 2014, Safehian and Ramezanianpour 2015).

Considerable research has been undertaken on corrosion-induced cracking of concrete cover, effective parameters on the process, and the time to cracking of the cover. The research can be classified into three main categories, experimental tests, analytical studies, and numerical simulations (Clark and Saifullah 1993, Andrade *et al.* 1996, Oh *et al.* 2009, Zhao *et al.* 2012, Morinaga 1988, Williamson and Clark 2000, Pantazopoulou and Papoulia 2001, Bhargava *et al.* 2006, Suda *et al.* 1993, Du *et al.* 2006, Chen and Mahadaven 2008, Ozbolt *et al.* 2011, Cao *et al.* 2013, German and Pamin 2015, Chen and Leung 2015).

There are two main test methods, in practice, to conduct the experiments, accelerated and simulated corrosion test methods (Clark and Saifullah 1993, Andrade *et al.* 1996, Oh *et al.* 2009, Zhao *et al.* 2012, Morinaga 1988, Williamson and Clark 2000). Andrade *et al.* (1993) and Rodriguez *et al.* (1996) employed the accelerated method for investigating the corrosion-induced cracking and influential parameters to develop equations for the time of concrete cover cracking. Localized corrosion effect of steel reinforcement on the

∗Corresponding author, Assistant Professor
E-mail: tadeh.zirakian@csun.edu
[a]M.Sc. Graduate
[b]Associate Professor
[c]Ph.D. Student

ISSN: 1225-4568 (Print), 1598-6217 (Online)

cracking was experimentally accelerated by Torres-Acosta and Sagüés (2004) where an empirical equation was also proposed for the time of cracking. McLeish (1986) experimentally simulated the pressure induced by reinforcing bars corrosion to examine the effective parameters on the cracking process. Allan and Cherry (1992) examined local corrosion of reinforcement through the simulated corrosion test method. Williamson and Clark (2000) carried out experimental tests by means of the simulated method to investigate the pressure magnitude induced by the corrosion products which would result in surface cracking of the concrete cover.

A variety of analytical models dealing with corrosion-induced concrete cover cracking can be found in the literature (Pantazopoulou and Papoulia 2001, Bhargava *et al.* 2006, Bazant 1979, Liu and Weyers 1998, Maaddawy and Soudki 2007, Lu *et al.* 2011, Yu 2013). Bazant (1979) proposed an analytical model to predict the time of the cover cracking caused by corrosion of embedded reinforcing steel. Another model was developed by Bhargava *et al.* (2006) to predict the time required for cover cracking and the weight loss of reinforcement. Yu (2013) used the damage mechanics with consideration of two distinct stages, i.e., the non-cracking stage and the partial cracking stage, to develop an analytical model for predicting the time of the concrete cracking.

Dagher and Kulendran (1992) simulated the corrosion-induced fracture of concrete via finite element analysis where smeared crack approach was employed for fracture analysis. The model considered only the radial expansive deformation around the reinforcing bar induced by corrosion while other loadings, such as dead and live loads, were not included. Du *et al.* (2006) presented a two-dimensional (2D) finite element (FE) model under a plane strain assumption to idealize three-dimensional physical specimens, tested by the simulated method and investigated the development mechanism of the concrete cracking. The model was then employed to predict test results from reinforced concrete accelerated corrosion. An integrated computational methodology for chloride-induced degradation assessment of RC structures by considering all three phases of the deterioration process, i.e., chloride penetration process, reinforcement corrosion, and rust expansion was developed by Chen and Mahadaven (2008). Finite element analysis with a smeared cracking approach was implemented to simulate the rust expansion and the associated concrete cracking process.

In this paper, the effect of various parameters including concrete cover thickness, C, reinforcing bar diameter, d, and concrete tensile strength, f_t, on the pressure required for cracking is investigated via eXtended Finite Element Method (XFEM) in ABAQUS software. Furthermore, using an empirical equation proposed by Martín-Pérez (1999) and also taking advantage of the developed numerical model, the required times for the cover cracking are estimated and then compared to the experimental data. Lastly, as a practical application of the numerical model, a parametric study is undertaken to determine the optimum ratio of the rebar diameter (d) to the reinforcing bars spacing (S) to avoid concrete cover delamination.

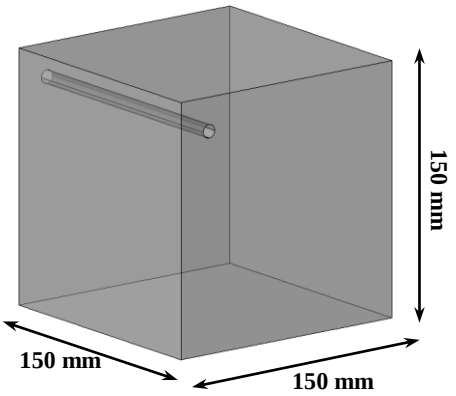

Fig. 1 Specimens' dimensions tested by Williamson and Clark (2000)

Table 1 Mechanical properties of concrete

Compressive strength, (MPa)	35
Tensile strength, f_t (MPa)	2.8
Poisson's ratio, (v)	0.2

2. Finite element modeling and verification

The concrete specimens have been modeled and analyzed using ABAQUS (Standard User's Manual, ver. 6.10 2010) finite element software. The eXtended Finite Element Method (XFEM) within the linear elastic fracture mechanics (LEFM) framework is incorporated in the nonlinear analysis of the models to capture concrete cover cracking. Taking advantage of XFEM feature, i.e. enriching degrees of freedom, crack initiation and propagation along an arbitrary and solution-dependent path with no requirement of re-meshing the models are achieved (Abdelaziz and Hamouine 2008, Asadpour and Mohammadi 2007, Areias and Belytschko 2005, Sukumar *et al.* 2001, Moes *et al.* 1999). The 8-noded solid element C3D8R is used to model concrete material.

The three-dimensional (3D) finite element model is verified through comparison of numerical results with the experimental data reported by Williamson and Clark (2000). The test specimens were cubes with edge length 150 mm and a cylindrical hole located at one corner with diameter of 8 mm, as seen in Fig. 1.

The ratios of concrete cover thicknesses to the hole diameter, i.e., C/d, were 0.5, 1.0, and 2.0. A uniform and gradually increasing outward internal pressure is applied into the holes to simulate the expansion induced by corrosion of steel bars. The mechanical properties of the concrete material are provided in Table 1 (Williamson and Clark 2000).

The modulus of elasticity of concrete, E_c, was not reported by Williamson and Clark (2000), hence four different values of E_c are considered for mesh sensitivity analysis and the following numerical validation. The mesh sensitivity analysis is performed on the required pressure ($P_{req.}$) for a model with C/d=0.5 and d=8 mm, to determine efficient mesh sizes. Based on mesh refinement studies, as seen in Fig. 2, the maximum element sizes less than 10 mm lead to negligible differences in $P_{req.}$, therefore maximum

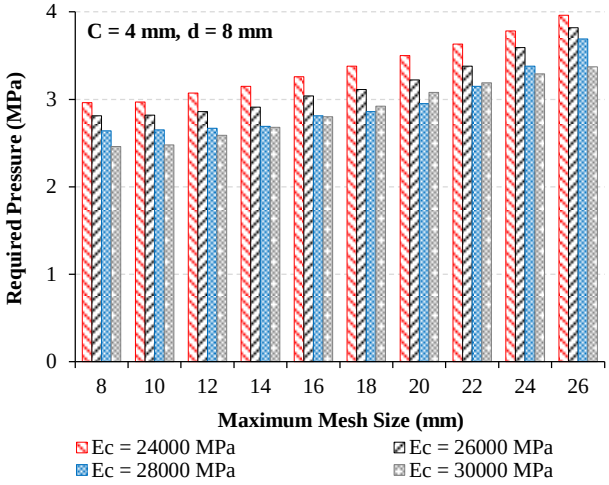

Minimum mesh size for all pattern is 1mm

Fig. 2 Mesh sensitivity analysis

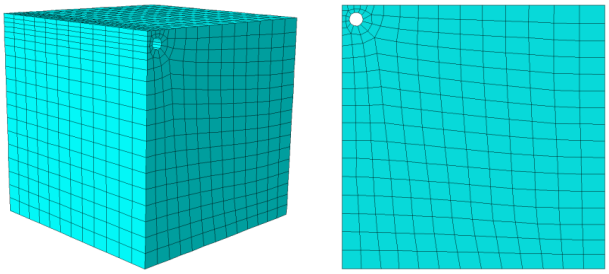

(a) Perspective view (b) Front view

C/*d*=0.5 and *d*=8 mm

Fig. 3 A typical finite element model of the concrete specimens

element size of 10 mm is considered for the meshing purposes. In the vicinity of the holes where stress concentration is high and prone to crack initiation, a finer mesh pattern is applied. Fig. 3 shows the model with *C*/*d*=0.5 and *d*=8 mm.

Since the actual modulus of elasticity was not reported by Williamson and Clark (2000), a sensitivity analysis is undertaken to estimate Young's modulus (E_c). Similar to the previous sensitivity study, the model with *C*/*d*=0.5 and *d*=8 mm is considered where the optimum mesh size is applied. The results are provided in Fig. 4. The experimental required pressure for the respective specimen is 2.65 MPa, hence Young's modulus of 28 GPa which results in the most accurate numerical result is considered for the following numerical validation and simulations.

In this paper, numerical models are labelled such that the concrete cover thickness (*C*), bar diameter (*d*), and tensile strength of concrete (f_t) of each model can be identified from the label. For example, the label "M-4-8-2.8" indicates that the model has a cover thickness of 4 mm, a hole with diameter of 8 mm, and concrete with tensile strength of 2.8 MPa.

Experimental results from the testing of three specimens are considered for the validation of the numerical simulation. Comparison of the results shown in Fig. 5 and tabulated in Table 2 demonstrates that the agreement

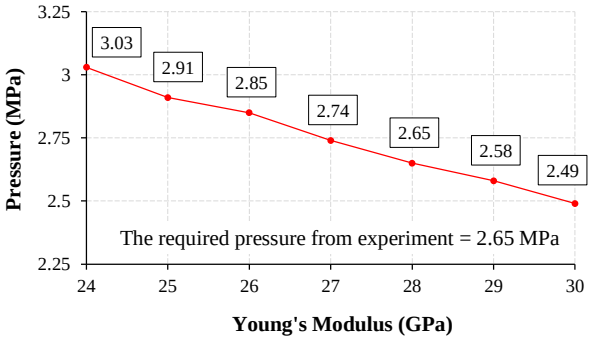

Fig. 4 Sensitivity analysis of Young's modulus

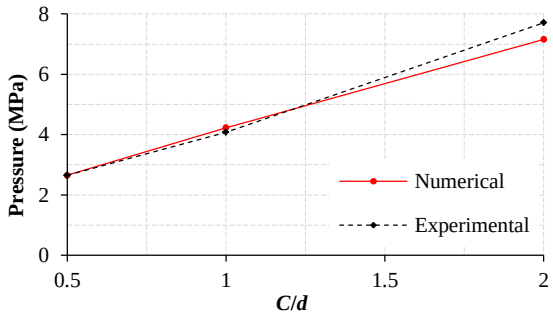

Fig. 5 Comparison of experimental and numerical results; variation of the required pressure for concrete cover cracking vs. *C*/*d*

Table 2 The required pressure for concrete cover cracking

Specimen ID	$P_{req./numerical}$ (MPa)	$P_{req./exp.}$ (MPa)	ΔP (%)
M-4-8-2.8	2.65	2.65	0.00
M-8-8-2.8	4.23	4.08	3.68
M-16-8-2.8	7.16	7.71	7.13

between experimental results and numerical predictions is by and large good, which is in turn indicative of validity of the numerical simulation. It should be noted that the failure pressure, i.e., $P_{req.}$, is defined as the maximum pressure sustained by specimen/model at cracking of the concrete cover.

In the testing of the specimens, uniform corrosion was simulated by using a hydraulic jack in order to pressurize a soft PVC tube inserted into the hollow concrete specimens. By means of a manual pump and a mounted pressure gauge, the specimens were incrementally loaded to failure. Accordingly, in the numerical modeling of the test specimens, the internal pressure of the hollow concrete model was used to simulate the expansive pressure developed due to uniform corrosion. This pressure was increased in increments of 0.01 MPa up to the failure of the numerical models.

3. Discussion of finite element results

The effects of parameters including concrete cover thickness (*C*), steel bar diameter (*d*), and tensile strength of concrete (f_t) on the required pressure for concrete cover

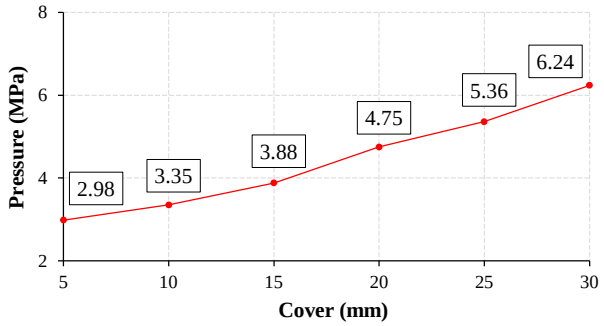

Fig. 6 Effect of concrete cover thickness on the required pressure for cracking

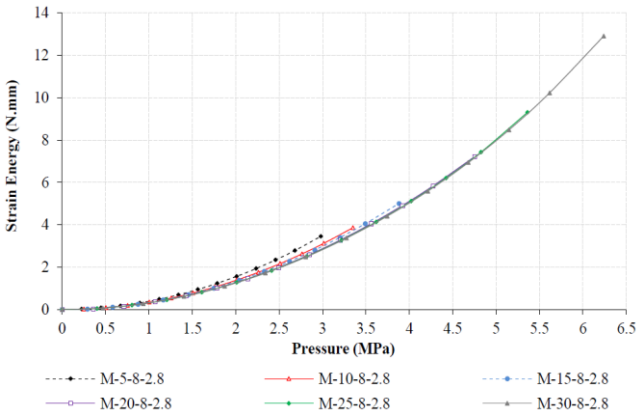

Fig. 7 Strain energy vs. the required pressure for cracking

cracking are investigated in this section.

3.1 Effect of concrete cover thickness

To evaluate the effect of the cover thickness variation on the required expansive pressure, six models are developed with varying cover thicknesses (C), from 5 mm to 30 mm while all other geometrical and material properties are kept constant (d=8 mm, f_t=2.8 MPa). Therefore, the models' labels are "M-C-8-2.8".

The results are provided in Fig. 6. As can be seen, by increasing the cover thickness, the required pressure is increased, i.e., the thicker the cover, the higher the pressure.

Fig. 7 shows the variation of strain energy versus pressure of the models up to the respective failure points.

The increasing of the cover thickness increases the failure pressure and consequently the ultimate strain energy. However, at the same pressure values, cover thickness increase leads to decrease in strain energy. It is likely attributable to the deformation pattern of the models. The deformation is localized at the vicinity of the areas with lower stiffness, i.e. concrete cover, where the cracking initiates. For a given pressure value, models with smaller cover thicknesses have bigger deformations mostly localized around the cover which consequently results in higher strain energies. By increasing of the cover, the surrounding areas of the rebar become more symmetric in stiffness which results in higher required pressure for deformation localization and crack initiation.

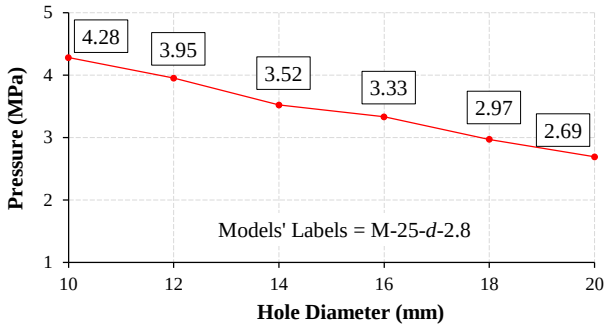

Fig. 8 Effect of hole diameter on the required pressure for cracking

Table 3 Effect of concrete tensile strength on the required expansive pressure

Model ID	C (mm)	d (mm)	C/d	f_t (MPa)	$P_{req.}$(MPa)
M-4-8-1.5	4	8	0.5		1.28
M-8-8-1.5	8	8	1	1.5	2.39
M-12-8-1.5	12	8	1.5		3.41
M-4-8-1.7	4	8	0.5		1.56
M-8-8-1.7	8	8	1	1.7	2.67
M-12-8-1.7	12	8	1.5		3.63
M-4-8-1.9	4	8	0.5		1.70
M-8-8-1.9	8	8	1	1.9	3.05
M-12-8-1.9	12	8	1.5		4.09
M-4-8-2.1	4	8	0.5		1.92
M-8-8-2.1	8	8	1	2.1	3.35
M-12-8-2.1	12	8	1.5		4.77

3.2 Effect of steel bar diameter

Six finite element models are developed with varying hole diameters (d), from 10 mm to 20 mm, where all other geometrical and material properties are kept constant (C=25 mm, f_t=2.8 MPa), hence the models' labels are "M-25-d-2.8".

The pressure required for cracking of the concrete cover for each model is shown in Fig. 8. As seen in the figure, the expansive pressure decreases as the hole diameter increases. By increasing of the hole diameter, the lateral surface of the hole increases which results in higher outward force and consequently lower required pressure for the cracking.

3.3 Effect of tensile strength of concrete

In this section, the effect of tensile strength of concrete (f_t) is investigated. To this end, four values for the tensile strength are examined (1.5 MPa, 1.7 MPa, 1.9 MPa, and 2.1 MPa) where for each value, three different cover thicknesses are considered. The required pressure for the cracking for all the models are provided in Table 3 and Fig. 9. As expected, the pressure increases with tensile strength increase.

As seen in Fig. 9, the required expansive pressure for cover cracking increases as the tensile strength increases, since increase in tensile strength raises the bearing capacity of the concrete cover.

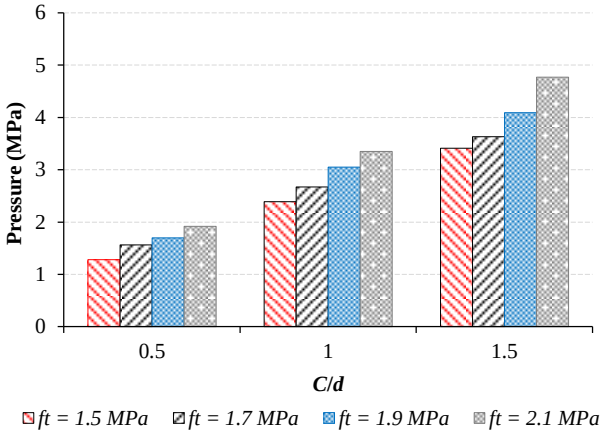

Fig. 9 Effect of concrete tensile strength on the required expansive pressure

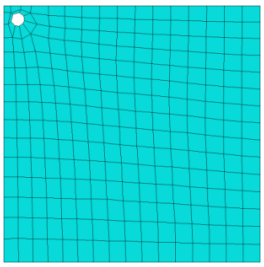

C/*d*=0.5 and *d*=8 mm

Fig. 10 A typical FE model of the concrete specimens

4. Development of an efficient two-dimensional model

To reduce the computational cost of 3D simulation, a two-dimensional (2D) finite element (FE) model is developed which is able to give results close to its 3D counterpart. The developed 2D model is based on a plane strain finite element formulation. The 4-noded bilinear shell element, i.e., CAX4R, is used for such plane strain simulations. A typical 2D finite element model is shown in Fig. 10. A mesh sensitivity analysis is undertaken to determine the maximum element size for such simplified models where a value of 28 GPa is considered for Young's modulus. It is found that the maximum element size of 10 mm results in reasonable accuracy in the simulation results.

The 2D model is validated through comparison of the numerical results with experimental counterpart used for the 3D model validation. Both 2D and 3D numerical results along with the respective experimental data are provided in Fig. 11. As seen, the 2D model can accurately predict the required pressure for initiation of concrete cover cracking where a relatively lower computational cost is needed.

5. Time prediction of concrete cover cracking

5.1 Concept and equations

To determine the time from corrosion initiation to concrete cover cracking, the empirical equation proposed by

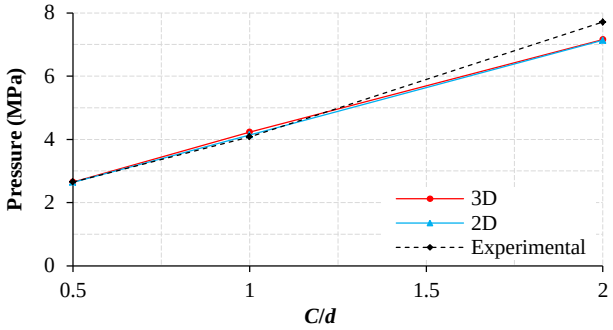

Fig. 11 Validation of 2D numerical model

Table 4 Risk of corrosion

Risk of Corrosion	i_{corr} ($\mu A/cm^2$)
Negligible	$i_{corr} < 0.1$
Low	$0.1 < i_{corr} < 0.5$
Middle	$0.5 < i_{corr} < 1.0$
High	$i_{corr} > 1.0$

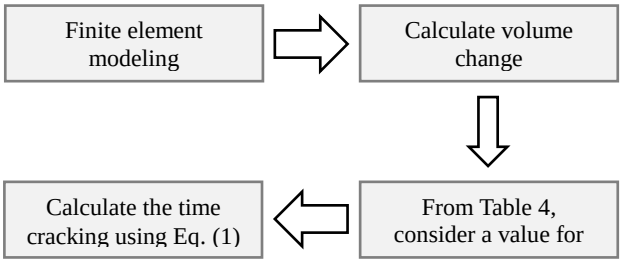

Fig. 12 Calculation procedure of the cracking time

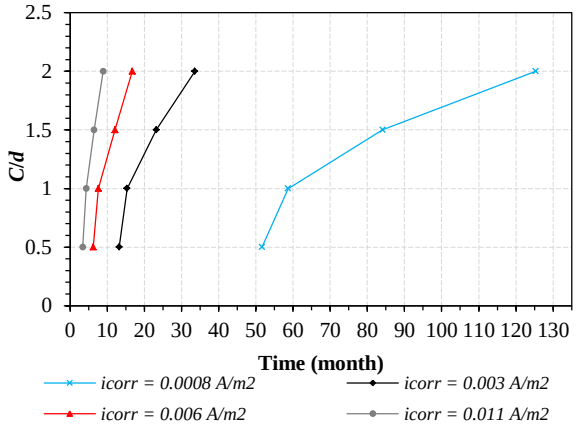

Fig. 13 Risk of corrosion

Martín-Pérez (1999) is employed (Eq. (1)).

$$\Delta V_s = 3.6466 \times 10^{-11}\, \pi\, d_b\, i_{corr}\, \Delta t \qquad (1)$$

where i_{corr} is the rate of corrosion ($\mu A/cm^2$), ΔV_s is the volume change of steel, d_b is the bar diameter (m), and Δt is the time (s). The risk of corrosion is divided into four levels as provided in Table 4 which depending on the iron oxidation level, corrosion leads to varying corrosion current density (i_{corr}) which directly influences the volume change.

Fig. 12 shows the procedure how to employ the numerical model to predict the time from corrosion

Table 5 Experimental specimens' characteristics

Specimen	d (mm)	C (mm)	i_{corr} ($\mu A/cm^2$)	f_t (MPa)	E_c (GPa)
Andrade *et al*. (1996)	16	20	100	3.55	22
Rodriguez *et al*. (1996)	16	20	100	3.85	22
Maaddawy and Soudki (2007)	16	33	150	4.9	28

Table 6 The predicted and experimental time for cracking

Specimen	Experimental time (h)	Predicted time (h)	Dif. (%)
Andrade *et al*. (1996)	96	117	17.95
Rodriguez *et al.* (1996)	113	153	26.14
Maaddawy and Soudki (2007)	95	121	21.48

initiation to cover cracking using the empirical equation, i.e. Eq. (1).

Fig. 13 shows the concrete cover to bar diameter ratio versus time to the cover cracking obtained from numerical simulation and the empirical equation for four different values of i_{corr}. From the figure, the required time for the concrete cover cracking decreases as i_{corr} increases. Moreover, the required time increases as the C/d ratio increase.

5.2 Accuracy of the predicted time

To assess the accuracy of the time estimation, the results from experiments in the literature and the predicted data are compared. The experimental specimens' properties (C, d, i_{corr}) are provided in Table 5. In some cases where the actual tensile strength (f_t) and the modulus of elasticity (E_c) are not available, they are estimated by using Eqs. (2) and (3), respectively, in accordance with ACI 318 (2011).

$$f_t = 0.33 \times \sqrt{f_c'} \quad (MPa) \tag{2}$$

$$E_c = 4730 \times \sqrt{f_c'} \quad (GPa) \tag{3}$$

The predicted times from corrosion initiation to concrete cover cracking are compared to the respective experimental data in Table 6.

As can be seen from the table, the experimental data to some extent are lower than the predicted values using the model. The difference between the cracking times obtained from numerical simulations and experiments could be attributed to the fact that experimental specimens generally have initial cracks mainly due to shrinkage and creep while no imperfection, i.e. pre-cracking, is assumed for the numerical models. Therefore, cracking times in the models are greater than those of the specimens.

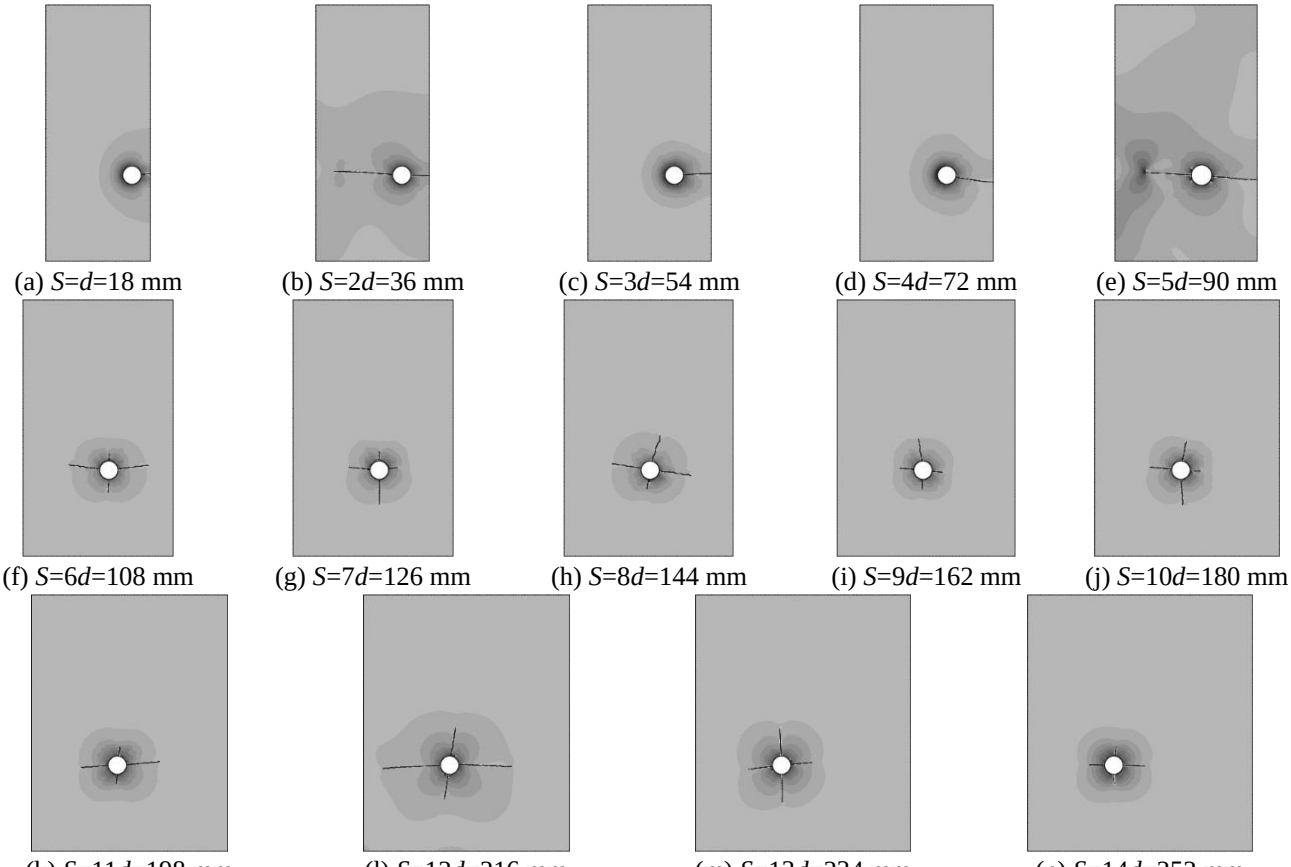

(a) S=d=18 mm (b) S=2d=36 mm (c) S=3d=54 mm (d) S=4d=72 mm (e) S=5d=90 mm

(f) S=6d=108 mm (g) S=7d=126 mm (h) S=8d=144 mm (i) S=9d=162 mm (j) S=10d=180 mm

(k) S=11d=198 mm (l) S=12d=216 mm (m) S=13d=234 mm (n) S=14d=252 mm

Fig. 14 Cover cracking pattern for varying S/d ratio

Table 7 The required pressure for crack initiation and time for cracking

Parameters	2Φ26	3Φ22	4Φ18	5Φ16	8Φ14
P_{cr} (MPa)	18.5	14.65	13.5	10.3	15.35
Δt (Month)	4.8	5.4	5.9	6.6	7.3

6. Failure mode of cracking

In the preceding sections, required pressure for concrete cover cracking due to corrosion and the time to cracking of the cover were evaluated. In this section, failure mode of cracking for a given section, induced by corrosion is investigated. According to the exposure condition of RC structures, design codes and guidelines recommend a minimum cover thickness. In general, there are two distinct failure modes for cover cracking, i.e., spalling and delamination; however, there is no constraint on the rebar spacing (Jamali *et al*. 2013).

The cover cracking patterns for a section having 2 steel bars (Φ18) with varying rebar spacing (S) are Presented in Fig. 14.

The height of the section (H) and cover thickness (C) are 250 mm and 75 mm, respectively, and the width of the sections equals $2\times(C+d)+S$. By taking advantage of the symmetry in geometry and loading of the models, left side of the models with consideration of proper boundary conditions is modeled.

From the results, for a perfectly homogenous concrete and perfectly uniform build-up of corrosion products around the reinforcing bars, the mode of failure depends on the rebar spacing and diameter. It is evident that for S/d ratios less than 6 the failure mode of cracking is delamination.

In the following, as an example, the favorable arrangement of reinforcement bars of a section with dimensions ($W\times H$) of 400×500 mm, cover thickness (C) of 75 mm, and reinforcement ratio (ρ) of 0.5% is determined in order to avoid cover delamination. Available reinforcing bars are Φ14, Φ16, Φ18, Φ22, and Φ26. The environment is considered to be highly aggressive. Also, i_{corr} is considered to be equal to 0.011 A/m^2.

Firstly, the required pressure for crack initiation and time to cracking of 5 different configurations are determined and summarized in Table 7. Secondly, the cracking pattern of the models after 7.3 months is predicted and shown in Fig. 15.

Models with 3Φ22 bars (Fig. 15(b)), 4Φ18 bars (Fig. 15(c)), and 5Φ16 bars (Fig. 15(d)) show delamination pattern for cover cracking, while in cases of the models with 2Φ26 bars (Fig. 15(a)) and 8Φ14 bars (Fig. 15(e)) the cracks propagate in both horizontal and vertical directions. By comparing the required pressure and the time to cracking of the two models with 2Φ26 and 8Φ14 bars from Table 7, the latter which possesses a relatively higher time, i.e., the model with 8Φ14 bars and shown in Fig. 15(e), is chosen as the model with favorable reinforcement arrangement.

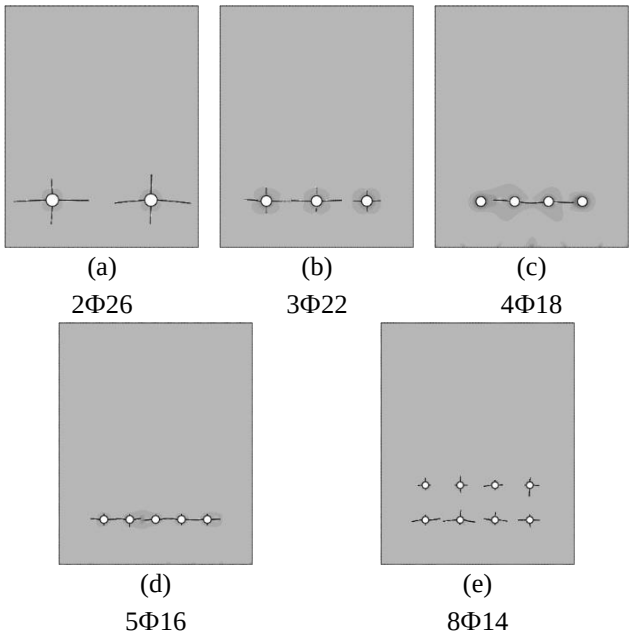

Fig. 15 Reinforcement arrangement of a section

7. Conclusions

This paper presents generic 2D and 3D XFEM models to simulate the concrete cover cracking due to internal expansive pressure induced by steel reinforcing bars corrosion. Based on the results and findings of this study, the following conclusions can be drawn:

1) Increase in concrete cover thickness and tensile strength raises the required pressure for cover cracking, while increase in bar diameter decreases the required pressure.

2) The volume change of steel (ΔV_s) can be obtained from numerical simulation instead of experiment, and used along with the empirical equations, e.g., Eq. (1) proposed by Martín-Pérez (1999), in order to predict the required time for cracking.

3) The 2D model can be employed to determine section configurations in order to achieve desirable cracking characteristics in terms of pattern, i.e. spalling and delamination, and the required pressure as well as the time for cracking.

References

ABAQUS (2011), ABAQUS Documentation, Dassault Systèmes, Providence, Rhode Island, USA.

Abdelaziz, Y. and Hamouine, A. (2008), "A survey of the extended finite element", *Comput. Struct.*, **86**(11-12), 1141-1151.

ACI 318 (2011), Building Code Requirements for Structural Concrete (ACI 318-11) and Commentary, American Concrete Institute, Farmington Hills, MI, USA.

Allan, M.L. and Cherry B.W. (1992), "Factors controlling the amount of corrosion for cracking in reinforced concrete", *Corros.*, **48**(5), 426-430.

Andrade, C., Alonso, C. and Molina, F.J. (1993), "Cover cracking as a function of bar corrosion: Part I-Experimental test", *Mater. Struct.*, **26**(8), 453-464.

Andrade, C., Alonso, C., Rodriguez, J. and Garcia, M. (1996), "Cover cracking and amount of rebar corrosion: importance of the current applied accelerated tests", *Proceedings of the International Conference on Concrete Repair, Rehabilitation and Protection*, London, UK, June.

Areias, P.M.A. and Belytschko, T. (2005), "Analysis of three-dimensional crack initiation and propagation using the extended finite element method", *Int. J. Numer. Meth. Eng.*, **63**(5), 760-788.

Asadpour, A. and Mohammadi, S. (2007), "Developing new enrichment functions for crack simulation in orthotropic media by the extended finite element method", *Int. J. Numer. Meth. Eng.*, **69**(10), 2150-2172.

Bazant, Z.P. (1979), "Physical model for steel corrosion in sea structures-applications", *J. Struct. Div.*, **105**(6), 1155-1166.

Bhargava, K., Ghosh, A.K., Mori, Y. and Ramanujam S. (2006), "Model for cover cracking due to rebar corrosion in RC structures", *Eng. Struct.*, **28**(8), 1093-1109.

Broomfield, J.P. (2007), *Corrosion of Steel in Concrete: Understanding, Investigation and Repair*, 2nd Edition, CRC Press, Taylor & Francis Group, London, UK.

Cao, C., Cheung, M.M.S. and Chan, B.Y.B. (2013), "Modeling of interaction between corrosion-induced concrete cover crack and steel corrosion rate", *Corros. Sci.*, **69**, 97-109.

Chen, D. and Mahadaven, S. (2008), "Chloride-induced reinforcement corrosion and concrete cracking simulation", *Cement Concrete Res.*, **30**(3), 227-238.

Chen, E. and Leung C.K.Y. (2015), "Finite element modeling of concrete cover cracking due to non-uniform steel corrosion", *Eng. Fract. Mech.*, **134**, 61-78.

Clark, L.A. and Saifullah M. (1993), "Effect of corrosion on reinforcement bond strength", *Proceedings of the 5th International Conference on Structural Faults and Repairs*, Edinburgh, UK, June.

Dagher, H.J. and Kulendran, S. (1992), "Finite element modeling of corrosion damage in concrete structures", *ACI Struct. J.*, **89**(6), 699-708.

Du, Y.G., Chan, A.H.C. and Clark, L.A. (2006), "Finite element analysis of the effects of radial expansion of corroded reinforcement", *Comput. Struct.*, **84**(13-14), 917-929.

German, M. and Pamin, J. (2015), "FEM simulations of cracking in RC beams due to corrosion progress", *Arch. Civ. Mech. Eng.*, **15**(4), 1160-1172.

http://dx.doi.org/10.1016/j.acme.2014.12.010.

Jamali, A., Angst, U., Adey, B. and Elsener, B. (2013), "Modeling of corrosion-induced concrete cover cracking: A critical analysis", *Constr. Build Mater.*, **42**, 225-237.

Liu, Y. (1996), "Modeling the time to corrosion cracking of the cover concrete in chloride contaminated reinforced concrete structures", Ph.D. Dissertation, Department of Civil Engineering, Virginia Polytechnic Institute and State University, Blacksburg, Virginia, USA.

Liu, Y. and Weyers, R.E. (1998), "Modeling the time-to-corrosion cracking in chloride contaminated reinforced concrete structures", *ACI Mater. J.*, **95**(6), 675-680.

Lu, C., Jin, W. and Liu, R. (2011), "Reinforcement corrosion-induced cover cracking and its time prediction for reinforced concrete structures", *Corros. Sci.*, **53**(4), 1337-1347.

Maaddawy, T.E. and Soudki, K. (2007), "A model for prediction of time from corrosion initiation to corrosion cracking", *Cement Concrete Compos.*, **29**(3), 168-175.

Martín-Pérez, B. (1999), "Service life modelling of R.C. highway structures exposed to chlorides", Ph.D. Dissertation, Department of Civil Engineering, University of Toronto, Toronto, Canada.

McLeish, A. (1986), "Cracking due to corrosion", Taywood Engineering, Technical Note No. 1632.

Moes, N., Dolbow J. and Belytschko T. (1999) "A finite element method for crack growth without remeshing", *Int. J. Numer. Meth. Eng.*, **46**(1), 131-150.

Morinaga, S. (1988), "Prediction of service life of reinforced concrete building based on rate of corrosion of reinforcing steel", Special Report of Institute of Technology, Shimizu Corporation, Tokyo, Japan.

Oh, B.H., Kim, K.H. and Jang, B.S. (2009), "Critical corrosion amount to cause cracking of reinforced concrete structures", *ACI Mater. J.*, **106**(4), 333-339.

Ozbolt, J., Balabanic, G. and Kuster, M. (2011), "3D Numerical modeling of steel corrosion in concrete structures", *Corros. Sci.*, **53**(12), 4166-4177.

Pantazopoulou, S.J. and Papoulia, K.D. (2001), "Modeling cover-cracking due to reinforcement corrosion in RC structures", *J. Eng. Mech.*, ASCE, **127**(4), 342-351.

Rodriguez, J., Ortega, L.M., Casal, J. and Diez, J.M. (1996), "Corrosion of reinforcement and service life of concrete structures", *Proceedings of the 7th International Conference on Durability of Building Materials and Components*, Stockholm, Sweden.

Safehian, M. and Ramezanianpour, A.A. (2015), "Prediction of RC structure service life from field long term chloride diffusion", *Comput. Concrete*, **15**(4), 589-606.

Song, Z., Jiang, L., Chu, H., Xiong, C., Liu, R. and You, L. (2014), "Modeling of chloride diffusion in concrete immersed in CaCl2 and NaCl solutions with account of multi-phase reactions and ionic interactions", *Constr. Build Mater.*, **66**, 1-9.

Suda, K., Misra, S. and Motohashi, K. (1993), "Corrosion products of reinforcing bars embedded in concrete", *Corros. Sci.*, **35**(5-8), 1543-1549.

Sukumar, N., Chop, D.L., Moes, N. and Belytschko, T. (2001), "Modeling holes and Inclusions by Level sets in Extended Finite Element Method", *Comput. Method Appl. M.*, **190**(46-47), 6183-6200.

Torres-Acosta, A.A. and Sagüés, A.A. (2004), "Concrete cracking by localized steel corrosion-geometric effects", *ACI Mater. J.*, **101**(6), 501-507.

Tsao, W.H., Huang, N.M. and Liang, M.T. (2015), "Modelling of chloride diffusion in saturated concrete", *Comput. Concrete*, **15**(1), 127-140.

Williamson, S.J. and Clark, L.A. (2000), "Pressure required to cause cover cracking of concrete due to reinforcement corrosion", *Mag. Concrete Res.*, **52**(6), 455-467.

Yu, J. (2013) "Damage analysis and experimental study of reinforced concrete structures with rebar corrosion", Ph.D. Dissertation, Zhejiang University, Hangzhou, China.

Zhao, Y., Dong, J., Wu, Y., Wang, H., Li, X. and Xu, Q. (2014), "Steel corrosion and corrosion-induced cracking in recycled aggregate concrete", *Corros. Sci.*, **85**, 241-250.

Zhao, Y., Yu, J. and Jin, W. (2011), "Damage analysis and cracking model of reinforced concrete structures with rebar corrosion", *Corros. Sci.*, **53**(10), 3388-3397.

Zhao, Y., Yu, J., Hu, B. and Jin, W. (2012), "Crack shape and rust distribution in corrosion-induced cracking concrete", *Corros. Sci.*, **55**, 385-393.

CC